Unfolding and refolding properties of S pili on extraintestinal pathogenic Escherichia coli

Mickaël Castelain, A. E. Sjostrom, E. Fallman, B. E. Uhlin, M. Andersson

Eur Biophys J
DOI 10.1007/s00249-009-0552-8

ORIGINAL PAPER

Unfolding and refolding properties of S pili on extraintestinal pathogenic *Escherichia coli*

Mickaël Castelain · Annika E. Sjöström · Erik Fällman · Bernt Eric Uhlin · Magnus Andersson

Received: 14 May 2009 / Revised: 2 October 2009 / Accepted: 9 October 2009

Abstract S pili are members of the chaperone-usher-pathway-assembled pili family that are predominantly associated with neonatal meningitis (S_{II}) and believed to play a role in ascending urinary tract infections (S_I). We used force-measuring optical tweezers to characterize the intrinsic biomechanical properties and kinetics of S_{II} and S_I pili. Under steady-state conditions, a sequential unfolding of the layers in the helix-like rod occurred at somewhat different forces, 26 pN for S_{II} pili and 21 pN for S_I pili, and there was an apparent difference in the kinetics, 1.3 and 8.8 Hz. Tests with bacteria defective in a newly recognized *sfa* gene ($sfaX_{II}$) indicated that absence of the $sfaX_{II}$ gene weakens the interactions of the fimbrium slightly and decreases the kinetics. Data of S_I are compared with those of previously assessed pili primary associated with urinary tract infections, the P and type 1 pili. S pili have weaker layer-to-layer bonds than both P and type 1 pili, 21, 28 and 30 pN, respectively. In addition, the S pili kinetics are ~10 times faster than the kinetics of P pili and ~550 times faster than the kinetics of type 1 pili. Our results also show that the biomechanical properties of pili expressed ectopically from a plasmid in a laboratory strain (HB101) and pili expressed from the chromosome of a clinical isolate (IHE3034) are identical. Moreover, we demonstrate that it is possible to distinguish, by analyzing force-extension data, the different types of pili expressed by an individual cell of a clinical bacterial isolate.

Keywords Fimbriae · Uropathogenic *Escherichia coli* · Bond breaking · Unfolding · Optical tweezers

Introduction

Extraintestinal pathogenic *Escherichia coli* (ExPEC) are known to be able to express a variety of flexible adhesion organelles, referred to as pili or fimbriae. Even though each single bacterium has the potential to express several different pili, it seldom produces more than one type of pili simultaneously presumably because of regulation in response to signals from the surrounding environment (as reviewed by Holden and Gally 2004). A rationale for the bacterium to express several types of pili is that different pili bind to different receptors expressed on the host tissue. For example S, P, and type 1 fimbrial adhesins specifically recognize α-sialyl-2,3-galactose (Parkkinen et al. 1986), Gal(α1-4)βGal (Lund et al. 1987), and α-D-mannoside receptors (Old 1972), respectively. Recent studies have shown that the adhesive potential of bacteria is not solely given by the properties of the adhesin molecules located at the distal end of the adhesion organelles; it can be strongly influenced also by the biomechanical properties of the pilus shaft structure constituting the main part of adhesion organelles (Duncan et al. 2005). A full understanding of bacterial adhesion therefore requires that we improve our

Erik Fällman: Deceased June 2008.

M. Castelain · E. Fällman · M. Andersson
Department of Physics, Umeå University, 901 87 Umea, Sweden

A. E. Sjöström · B. E. Uhlin (✉)
Department of Molecular Biology,
The Laboratory for Molecular Infection Medicine Sweden (MIMS), Umeå University, 901 87 Umea, Sweden
e-mail: bernt.eric.uhlin@molbiol.umu.se

M. Andersson (✉)
The Niels Bohr Institute,
University of Copenhagen, Copenhagen, Denmark
e-mail: magnus.andersson@physics.umu.se

Published online: 03 November 2009

knowledge about both the biomechanical and adhesive properties of attachment organelles.

The most studied pili, P pili (pyelonephritis-associated pili) and type 1 pili, characterized with respect to their three-dimensional structure and intrinsic mechanical properties (Andersson et al. 2007; Fällman et al. 2005), are commonly found on uropathogenic *E. coli* (UPEC). It has recently been shown that these helix-like structures, ~7-nm thick and ~1–2-μm long, possess large flexibility, mainly originating from their quaternary architecture (Jass et al. 2004). The quaternary structure is assembled from $\sim 10^3$ subunits that are linked head-to-tail via a donor strand exchange where the subunit donates its amino terminal extension to complete the fold of its neighbor (Sauer et al. 1999). These subunits are ordered in a helix-like sequence where the layer is connected to an adjacent layer via layer-to-layer interactions.

The quaternary structure of the pilus can be unfolded by unzipping the layers and thereby elongating the fimbrium. This action helps several pili share the shear forces caused by, e.g., the rinsing action of the urine, and it is hypothesized that this property controls the load on the adhesin and thereby optimizes the bond lifetime of, for instance, the FimH-mannose (Forero et al. 2006) and the PapG-galabiose (Björnham et al. 2009) interactions. If the action is performed under steady state, the unfolded structure can refold to its original configuration without dissipating energy (Andersson et al. 2008). The unfolding/refolding can also be a repeat action, meaning that the pili may be suggested to work as active dampers for shear forces (Andersson et al. 2006b). We have previously defined the extension behavior, i.e., the unfolding response to force by designating three separate regions that give rise to distinct differences in behavior (Andersson et al. 2008; 2006c; Jass et al. 2004). The first extension response (region I) shows a linear increase in force that indicates an elastic stretching of the layers. The second part (region II) corresponds to the unzipping of the layers that gives rise to a constant force-extension response. The third part (region III) shows a pseudo-elastic response that is similar to a worm-like chain model including a phase transition of the individual units that gives a smooth transition in the force-extension curve.

S pili can bind to human bladder and kidney epithelium and are predominantly correlated with neonatal meningitis caused by newborn meningitis *E. coli* (NMEC). In addition, they are also found in UPEC isolates and may have a role in ascending urinary tract infections (Wright and Hultgren 2006). S pili are expressed from polycistronic gene clusters, and the sfa_I and sfa_{II} pili operons characterized in ExPEC strains 536 (Berger et al. 1982; Hacker et al. 1985) and IHE3034 (Hacker et al. 1993) represent cases of S pili associated with urinary tract infection and meningitis, respectively. In spite of slightly different amino acid compositions of the respective subunits in the operons, both variants of S pili recognize the α-Sialyl-2,3-galactose receptor. In the quest of extending the knowledge about the physical properties and the divergence among different pili expressed by ExPEC, we have characterized the mechanical behavior of the two different S pili with force-measuring optical tweezers (FMOT). The high-force resolution of FMOT allows for detailed characterization of a single pilus, whereby we can assess the kinetics at a single polymer level. Prompted by the difference in kinetics observed for P and type 1 pili, we set out to characterize the properties of S pili to enable a comparison with P and type 1 pili, whose biogenesis, structure, and biological functions nevertheless are similar (Berglund and Knight 2003; Knight et al. 2002).

Materials and methods

Bacterial strains

The *E. coli* strains used in this study are shown in Table 1. The strains were grown at 37°C on solid L broth containing 1.5% agar, complemented with carbenicillin, Cb (50 μg/ml), when necessary. The clinical isolate was grown statically in brain-heart infusion (BHI) medium at 37°C when type 1 fimbriation was examined.

Construction of plasmids

Molecular genetics manipulations were performed essentially as described by Sambrook et al. (Sambrook and Russel 2001). The *Bam*HI-*Sal*I fragments with the $sfaX_{II}$ mutated genes from both pASS1 and pASS4 plasmids were cloned into the suicide vector pKO3. The resulting plasmids were introduced into MG1655/pAZZ50. As described by Guzman et al. (1995), the resulting plasmids pAES7 ($sfaX_{II}$*::kan*) and pAES8 ($\Delta sfaX_{II}$) were obtained by homologous recombination.

Atomic force microscopy (AFM)

Imaging of bacterial pili using AFM was done essentially as described earlier with some modifications (Balsalobre et al. 2003). Bacterial cells from solid medium were suspended in 50 μl filtered water before 10 μl was placed onto freshly cleaved ruby red mica (Goodfellow Cambridge Ltd, Cambridge, UK). The cells were incubated for 5 min at room temperature and blotted dry before being placed into a dessicator for a minimum of 2 h. Images were collected in a Nanoscope V AFM (Veeco software) using TappingMode™ with standard silicon cantilevers oscillated at resonant frequency (270–305 kHz). Images were collected

Table 1 Strains and plasmids used in this study

Plasmids and strains	Relevant characteristics	References
IHE3034	NMEC clinical isolate, O18K1:H7, carrier of the sfa_{II} operon (S pili)	Korhonen et al. (1985)
HB101	Non-piliated	Boyer and Roulland (1969)
MG1655	F^- *ilvG rphI*	Guyer et al. (1980)
pAZZ50	sfa_{II} operon (S pili) from the NMEC clinical isolate IHE3034 cloned into pBR322, Cb^R	Hacker et al. (1993)
pANN801-13	sfa_I operon (S pili) with truncated $sfaX_I$ gene from the UPEC clinical isolate 536 cloned into pBR322, Cb^R	Hacker et al. (1985)
pPAP5	*pap* operon (P pili) from the UPEC clinical isolate J96 cloned into pBR322, Cb^R	Lund et al. (1988)
pPKL4	*fim* operon (type 1 pili) from *E. coli* K12 PC31 cloned into pBR322, Cb^R	Klemm et al. (1985)
pKO3	Suicide vector, *ori* M13, *sacB, repA*^{TS}, Cm^R	Guzman et al. (1995)
pASS1	pUC18, $sfaX_{II}$*::kan*, Cb^R, Km^R	Sjöström et al. (2009a)
pASS4	pUC18, $\Delta sfaX_{II}$, Cb^R	Sjöström et al. (2009a)
pAES7	pAZZ50, $sfaX_{II}$*::kan*, Cb^R, Km^R	This work
pAES8	pAZZ50, $\Delta sfaX_{II}$, Cb^R	This work

in air at a scan rate of approximately 0.5–1.5 Hz. The final images were flattened and/or plane fitted in both axes using Veeco software and presented in either height or amplitude (error) mode.

Sample preparation and optical tweezers force measurements

We used force-measuring optical tweezers to extend an individual pilus under both steady-state conditions and during dynamic force spectroscopy (DFS) measurements. Several extension/contraction and DFS measurements were performed with an experimental procedure under standardized conditions that earlier has been used for characterization of P and type 1 pili (Andersson et al. 2006a, c; Fällman et al. 2004). In a given bacterial sample, individual pili were stretched from different bacteria with a 3.0-μm semi-transparent bead that acted as a force transducer. All beads were individually calibrated prior to each single pilus measurement. Measurements were repeated with each bacterial strain on different occasions, and data sets from at least three separate experiments were collected. Unfolding forces and their respective standard deviations were obtained for each experiment.

Theory of unfolding a helix-like polymer

A detailed description of the force-extension behavior of pili is found in (Andersson et al. 2006c). However, a brief summary is given below. As mention above, pili are assembled from many subunits into a helical arrangement. In addition, the quaternary structure is held rigid via layer-to-layer bonds, whereas head-to-tail interactions create the backbone. This structural design gives a response to external forces that is different from those of other macromolecules. The main rod is made from the major subunits: SfaA, PapA, and FimA, for S, P, and type 1 pili, respectively (Knight et al. 2002). Unfolding of the rod at an arbitrary position in the interior of the rod is very improbable since this requires the opening of several bonds simultaneously (Andersson et al. 2008). Consequently, the rod will unfold in a sequential manner after an initial fracture. The net opening rate of the outermost bond and the force-extension behavior are well described via rate theories and a sticky-chain model (Andersson et al. 2006a, c). The rate equation for such opening under a force, F, is given as,

$$dN_B/dt = k_{AB}^{th} e^{F\Delta x_{AT}/kT} - k_{AB}^{th} e^{(\Delta V_{AB} - F\Delta x_{TB})/kT}, \quad (1)$$

where k_{AB}^{th} is the thermal bond opening rate, Δx_{AT} and Δx_{TB} are the bond lengths, i.e., the distance from the closed and open state to the transition barrier, and ΔV_{AB} is the bond energy. Finally, k is the Boltzmann factor and T the temperature. For steady-state conditions, the opening and closure rates are at balance, which leads to an analytic solution for the steady-state unfolding force, F_{UF}^{bal},

$$F_{UF}^{bal} = \Delta V_{AB}/\Delta x_{AB}, \quad (2)$$

where Δx_{AB} is the bond opening length of the layer-to-layer bond (Andersson et al. 2006c). For high extension speeds the refolding rate in Eq. 1 can be neglected, and the rate equation simplifies to an expression relating the unfolding force to the extension speed, $\dot{L}$, as

$$F_{UF}(\dot{L}) = kT/\Delta x_{AT} \ln(\dot{L}/\dot{L}^{th}), \quad (3)$$

where $\dot{L}^{th}$ is defined to be the *thermal extension speed*, given by $k_{AB}^{th}\Delta x_{AB}$ (Andersson et al. 2006a). It is thereby

possible to use unfolding force-extension speed data to assess characteristic properties of the pilus under study, e.g., the bond length and the thermal extension speed.

These parameters can be assessed via dynamic force spectroscopy measurements (DFS), where the pilus is extended a number of times at different speeds (Andersson et al. 2006a), or via relaxation experiments (Andersson et al. 2007), where the pilus is forced to respond with a high force through an extension at high speed after which the extension is halted and the relaxation process is analyzed. In DFS characterizations, the unfolding force is described by Eq. 3, whereas the relaxation process is described by

$$dF_{\mathrm{UF}}(t)/dt = -\dot{L}^{\mathrm{th}}\kappa(e^{F_{\mathrm{UF}}(t)\Delta x_{\mathrm{AT}}/kT} - e^{(\Delta V_{\mathrm{AB}} - F_{\mathrm{UF}}(t)\Delta x_{\mathrm{TB}})/kT}), \quad (4)$$

where κ is the elastic constant of the force transducer (Andersson et al. 2007). In this work we use both these methods to assess the specific parameters of the different S pili and compare them with the parameters assessed for P and type 1 pili (Andersson et al. 2007).

Results and discussion

Expression of S pili variants by *E. coli*

S pili are expressed by pathogenic *E. coli* and two different variants, $\mathrm{Sfa_I}$ and $\mathrm{Sfa_{II}}$ (here referred to as $\mathrm{S_I}$ and $\mathrm{S_{II}}$ pili, respectively), have been extensively studied by molecular genetics approaches in case of the ExPEC strains 536 (Berger et al. 1982; Hacker et al. 1985) and IHE3034 (Hacker et al. 1993). The gene organization and functions of the genes in the two *sfa* operons are the same, but there are some sequence differences at both DNA level and amino acid level (Fig. 1a,b). Interestingly, the pili biogenesis components (e.g., the SfaE chaperon and SfaF usher proteins) residing inside the bacterium are almost identical (96–100%), whereas the structural fimbrial subunits and the adhesin, i.e., SfaA, SfaH, and SfaS, exposed outside the bacterium show differences of 16–40%. As is shown in Fig. 1b, an alignment of the major structural pilus subunit sequences, the $\mathrm{SfaA_I}$ and $\mathrm{SfaA_{II}}$ subunits, reveals that there is a $\sim$20% difference at the amino acid level, whereas the $\mathrm{SfaX_I}$ and $\mathrm{SfaX_{II}}$ proteins are identical with the exception of only 2 out of 166 amino acid residues.

Force measurements on pili expressed by the clinical isolates IHE3034

The clinical *E. coli* isolate strain IHE3034 carries the genes to express $\mathrm{S_{II}}$, MatB, and type 1 pili (Korhonen et al. 1985; Pouttu et al. 2001; Selander et al. 1986). We grew this strain to promote expression of either $\mathrm{S_{II}}$ or type 1 pili and used FMOT to investigate and assess specific intrinsic parameters of the expressed pili. The studies on the IHE3034 strain were performed in the same way as earlier described by Andersson et al. (2007). By identifying parameters such as steady-state response and kinetic behavior, at the single pilus level, a typical set of curves was obtained. As can be seen in the right panels of Fig. 2a,b, two different curve profiles appeared. By comparing the force responses and parameter values to previously assessed curves of HB101/pPKL4, it was obvious that the curve in panel *A* corresponded to a type 1 pilus (Andersson et al. 2007). The large gap between the unfolding and refolding plateau indicates, as also mentioned in (Andersson et al. 2007), that the experiment is not performed at steady state. In addition to the curve in panel *A*, we suggested that the curve in panel *B* was a representation of an S pilus. The average unfolding force of the presumed type 1 pili expressed by the IHE3034 strain, shown in Fig. 2a and fitted with a Gaussian function, was assessed to 55 $\pm$ 4 pN, whereas the presumed unfolding force of $\mathrm{S_{II}}$ pili was assessed to 26 $\pm$ 1 pN. Pili expressed by the second isolate were also analyzed with immunoglobulin antibody labeling to verify the FMOT results with respect to actual presence of the S pili on the bacteria (data not shown).

Characterization of S pili under steady-state

In order to specifically examine and compare the properties of each type of pili in a common genetic background, we used the *E. coli* laboratory strain HB101 (that lacks genes for pilus biogenesis) as host for plasmids harboring fimbrial gene clusters cloned from different ExPEC isolates. Figure 1c shows four representative areas of HB101 bacteria expressing $\mathrm{S_I}$, $\mathrm{S_{II}}$, P, and type 1 pili, visualized with atomic force microscopy (AFM). From the images, it could be concluded that all pili were expressed ectopically in the host strain and that no distinct differences considering lengths and number expressed per cell could be observed.

A typical force-extension/contraction response of $\mathrm{S_{II}}$ pili expressed from the plasmid-borne sfa_{II} gene cluster (HB101/pAZZ50) under steady-state conditions is shown in the right panel of Fig. 2c. The data (black curve) represent (I) stretching of the coiled $\mathrm{SfaA_{II}}$ rod, (II) sequential opening of the layer-to-layer bonds, and (III) transitions of the head-to-tail bonds. Such a response was similar to those assessed for P and type 1 pili (Andersson et al. 2007; Lugmaier et al. 2008; Miller et al. 2006). The average steady-state unfolding force, i.e., the force required to break the layer-to-layer bonds between consecutive layers, was found to be 26 $\pm$ 1 pN, which is slightly lower than the values for P and type 1 pili, 28 $\pm$ 2 pN and 30 $\pm$ 2 pN,

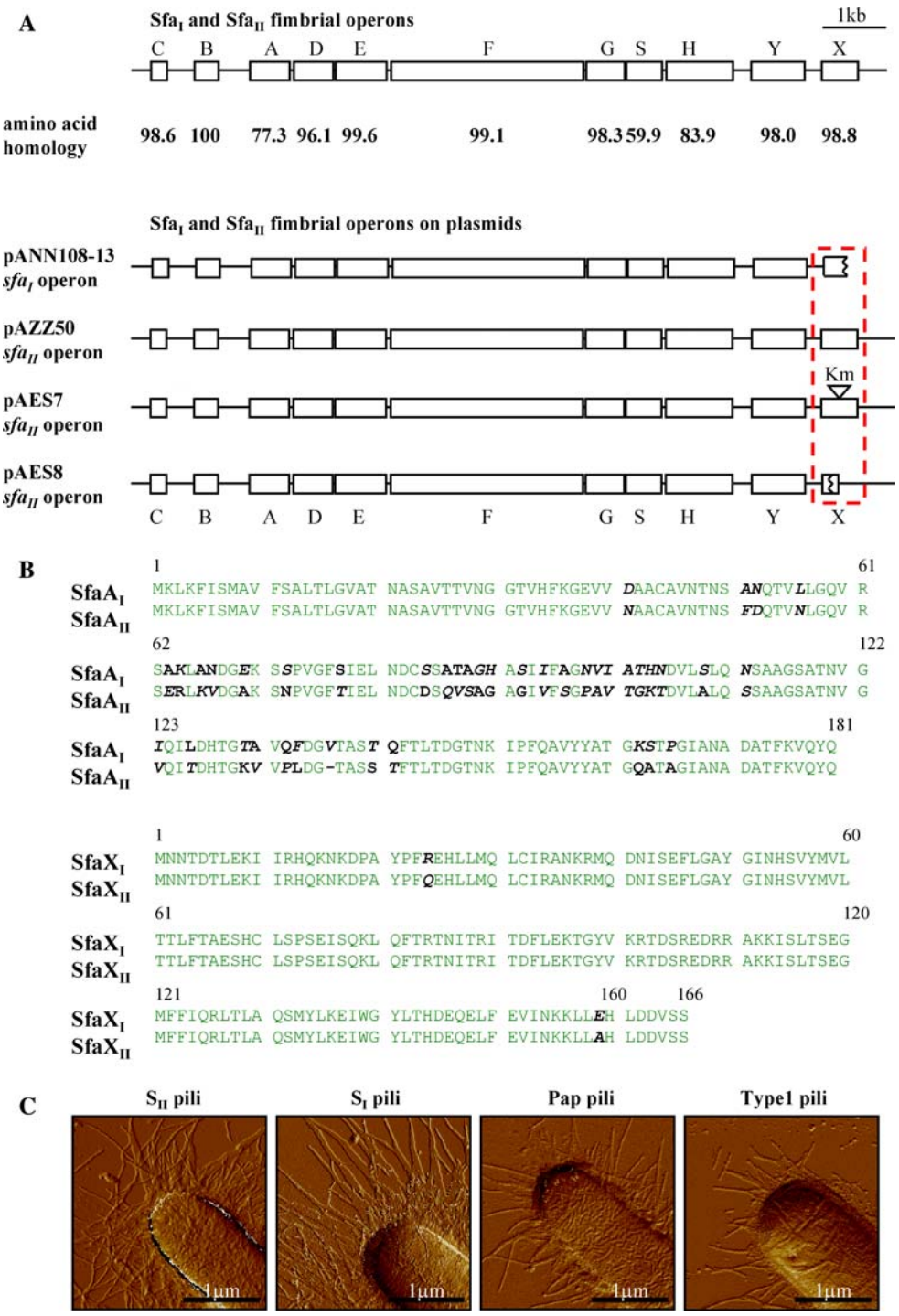

Fig. 1 **a** A schematic overview of the *sfa$_I$* and *sfa$_{II}$* fimbrial chromosomal operons [compilation based on sequence data and annotations (NCBI GenBank: CP000347; Brzuszkiewicz et al. 2006; Sjöström et al. 2009b)] and the *sfa$_I$*, *sfa$_{II}$*, *sfaX$_{II}$::kan*, and Δ*sfaX$_{II}$* plasmid borne operons. The calculated homology in percent at amino acid level is shown under the drawings of the chromosomal genes. The different alleles of the *sfaX* gene in the plasmid borne operons are highlighted by the *red box*. **b** Multiple sequence alignment (Corpet 1988) of the SfaA$_I$ and SfaA$_{II}$ major fimbrial subunit proteins (uppermost) and of the SfaX$_I$ and SfaX$_{II}$ (lowermost). *Green* residue combinations are identical. **c** AFM micrographs showing the different pili described in this study. The scanned area for each image was 5 by 5 µm^2

respectively (Andersson et al. 2008). Thus, the force required to break the layer-to-layer bonds are similar to that assessed for the clinical isolate cultured for S pili. The right panel of Fig. 2c shows multi-pili attachment to the bead. When separating the bacteria-bead system gently, the shortest and weakest attached pili will detach. Initially, four pili are attached, whereafter three detach, each event indicated with a + sign.

The green and red curves show two consecutive contraction patterns that represent refolding of the extended structure to its native form. As already shown for P and type 1 pili, refolding to the native form requires the formation of a nucleation kernel (Fällman et al. 2005; Lugmaier et al. 2008), i.e., after a pilus has been extended to a linearized form, it needs a certain amount of slack to reform the layer-to-layer interactions (Lugmaier et al. 2008). The sequential

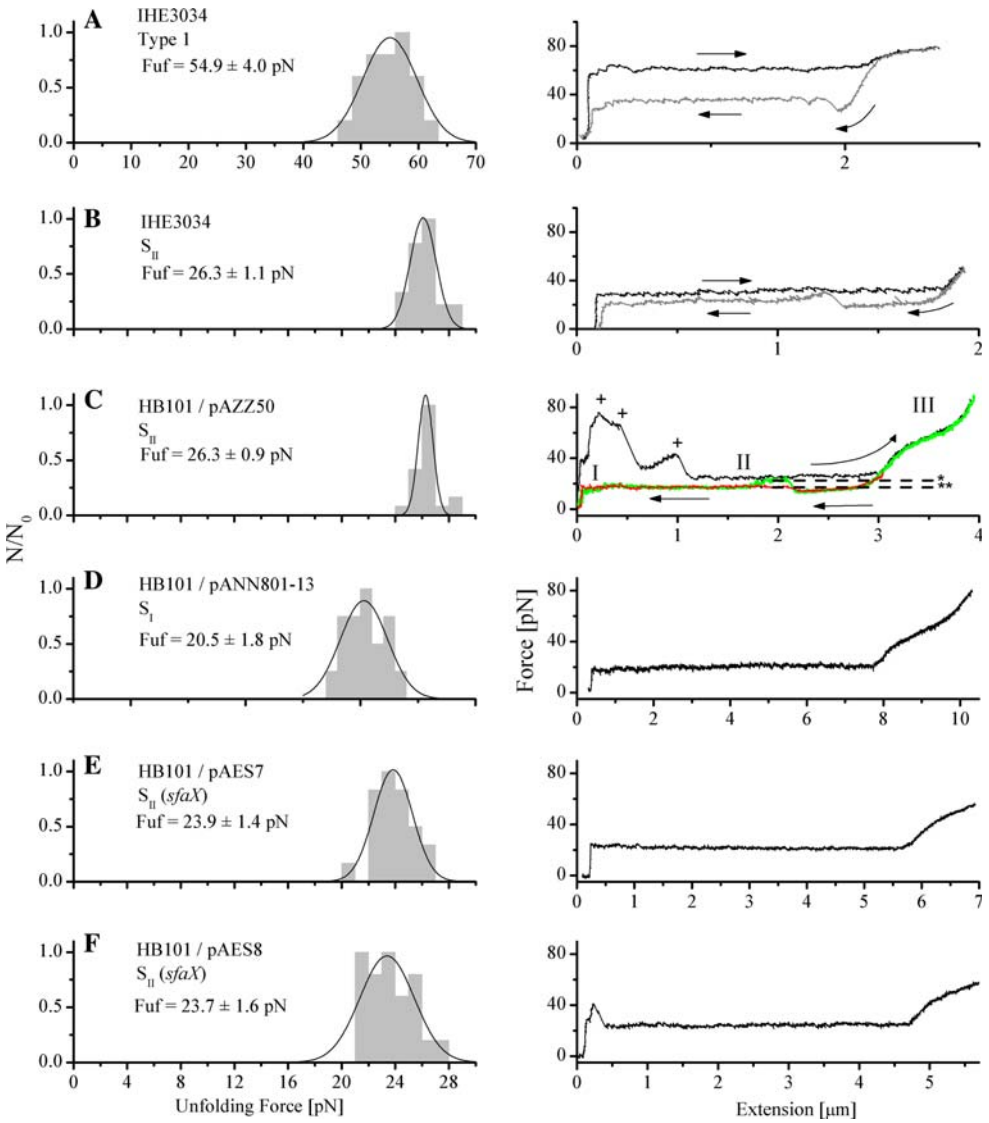

Fig. 2 Characterization of pili with force-measuring optical tweezers. The left side panels show the unfolding forces fitted with a Gaussian function (normalized distributions) for each respective strain. The right side panels represent force measurements of **a** wild-type bacteria IHE3034 expressing type 1 pili (*black curve*, unfolding; *grey curve*, refolding) and **b** wild-type bacteria IHE3034 expressing S pili (*black curve*, unfolding; *grey curve*, refolding). These two sets of curves do not show a complete region III response. The *arrows* indicate the direction of the applied force, i.e., the *right pointing arrow* indicates elongation, whereas the *left pointing arrow* indicates contraction of the pili. **c** A typical response from an S pilus, HB101/pAZZ50, under steady-state conditions. The *black curve* represents the unfolding sequence (the *initial peaks*, marked by +, are due to multi-pili interaction). The *red* and *green* (partly overlapping) *curves* show two consecutive refolding sequences. The characteristic unfolding regions I, II, and III are marked in the figure, and the two possible refolding levels are marked by * and **. **d** Unfolding response of the UTI correlated pili HB101/pANN801-13. *Panels E* and *F* are the unfolding responses of HB101/pAES7 and HB101/pAES8 pili, respectively

refolding can continue until all subunits are organized into a structure with the original helix-like shape. As shown in Fig. 2c, there was a distinct increase in force of ~10 pN at ~2.1 µm that indicated the creation of a nucleation kernel. Moreover, like the structure of type 1 pili, the S_{II} pili could refold at two different force levels, which is an indication of two possible configurations (Andersson et al. 2007). In the first cycle the pilus refolded at a force of ~18 pN (Fig. 2c; red line curve plot level marked with **), whereas in the subsequent cycle it initially refolded at ~23 pN (Fig. 2c; green line curve plot level marked with *) until it had contracted to ~1.8 µm. The refolding force then dropped and remained at ~18 pN.

To elucidate if there would be any detectable difference between S pili correlated to UTI and NMEC, we performed force-extension and kinetic response measurements of S_I pili encoded from the pANN801-13 plasmid clone. Not surprisingly, since the fimbrial components at protein level

and the presumed pili polymer architecture are almost identical, the force-extension under steady state appeared similar. A force-extension response from the S_I pili measurements is plotted in Fig. 2d, right panel. However, interestingly the average steady-state unfolding force was assessed to be 21 ± 2 pN, which is lower in comparison to that of the S_{II} pili.

Characterization of S pili with dynamic force spectroscopy

In order to find specific intrinsic parameters of these pili, we performed DFS measurements (Andersson et al. 2006a). The bond length of the layer-to-layer bonds, Δx_{AT}, and the corner velocities, $\dot{L}^*$, i.e., the extension speed above which the pilus shows a dynamic behavior, were analyzed. In the experiments, the unfolding region of a pilus was extended at 5, 10, 20, and 40 μm/s over a distance of 3 μm (Andersson et al. 2006a). The average unfolding forces of S_{II} are plotted and fitted to Eq. 3 (solid line), see Fig. 3a. Since the S_{II} pili can be extended under steady-state conditions for velocities under ∼0.4 μm/s, four data points are inserted in the figure for representative purpose. These are, however, not included in the fit.

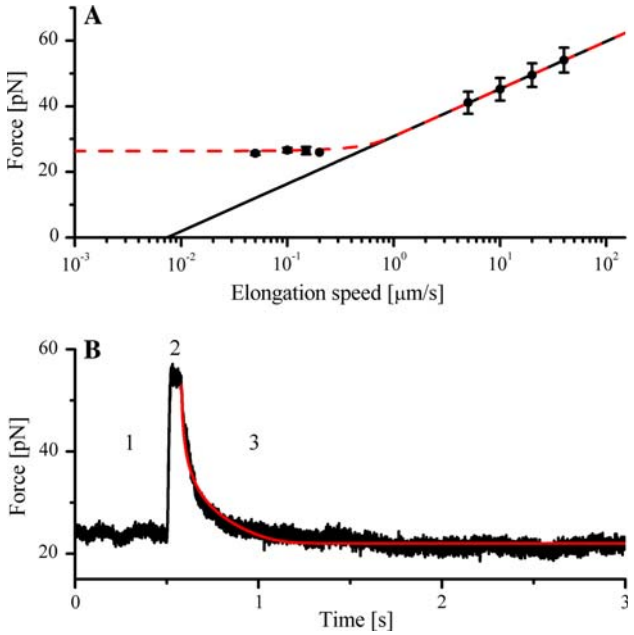

Fig. 3 **a** Dynamic force spectroscopy measurement of S_{II} pili. The rod was unfolded at 5, 10, 20, and 40 μm/s over a distance of 3 μm. The average fit of all data with Eq. 3 gave a bond length of 0.66 ± 0.08 nm and a corner velocity of 450 ± 150 nm/s. Unfolding forces taken under steady-state conditions (velocities <0.2 μm/s) are also included, and the *dashed red line* is a numeric simulation of Eq. 3 in (Andersson et al. 2006a). **b** The data were sampled during a relaxation measurement and fitted to Eq. 4. For this particular set of data, the bond length and the thermal bond opening rate of the subunits were assessed to 0.67 nm and 1.3 Hz, respectively

The average bond lengths of S_{II} and S_I pili were assessed to 0.66 ± 0.08 nm and 0.56 ± 0.14 nm, whereas the corner velocities were found to be 450 ± 150 nm/s and 700 ± 100 nm/s, respectively. The thermal bond opening rates were in turn assessed to 1.3 ± 0.9 Hz and 8.8 ± 5.3 Hz. Thus, the kinetics of S_I is ∼7 times higher than for S_{II}. These parameters are in the same regime as those assessed for P pili, i.e., 0.76 ± 0.11 nm, 400 ± 100 nm/s, and 0.8 ± 0.5 Hz, respectively (Andersson et al. 2006a). The corner velocity and thermal bond opening rate are on the other hand significantly different from those of type 1 pili, 6 ± 3 nm/s and 0.016 ± 0.009 Hz, whereas the bond length is similar, 0.59 ± 0.06 nm (Andersson et al. 2007).

To further illustrate kinetic divergences among pili, we performed relaxation measurements (Andersson et al. 2007). A typical relaxation process for an S_{II} pilus, extended under dynamic conditions, is shown in Fig. 3b. The measurement procedure was performed in the following sequence (1) the pilus is at steady state; (2) the pilus is extended at 40 μm/s, i.e., above the steady-state extension speed; (3) the extension is halted, whereafter the pilus relaxes to balance force. This method gives similar results as DFS measurements but visualizes the kinetic behavior of pili in an illustrative way. With a fit to Eq. 4, this particular curve gave a bond length and thermal bond opening rate of 0.66 ± 0.08 nm and 1.3 ± 0.9 Hz, which is in line with the parameter values assessed through DFS measurements.

As mentioned above, we assumed that the curve in Fig. 2b, right panel, represented a force-extension response of a S_{II} pilus from the IHE3034 bacteria. It was found that the average steady-state unfolding force of the pili expressed by that strain was 26 ± 1 pN. This is identical with the results presented above for S_{II} pili expressed by HB101/pAZZ50. In addition, the bond length and thermal bond opening rate were assessed to 0.66 ± 0.08 nm and 0.8 ± 0.4 Hz in the clinical isolate in comparison to 0.66 ± 0.08 nm and 1.3 ± 0.9 Hz for HB101/pAZZ50-expressed pili. We can therefore deduce that S_{II} pili expressed by two different strains—IHE3034 expressing S_{II} from the chromosome and HB101/pAZZ50 expressing S_{II} ectopically—show identical properties. Thus, the measurements indicate that the biomechanical properties of pili are not changed if the operons for pili biogenesis of a clinical isolate are implemented into the HB101 strain via a plasmid. It is therefore justified to use strain HB101 as a common model system for comparative studies of different pili types in a uniform strain background.

Differences in unfolding-refolding kinetics among different S pili

The S_I and S_{II} pili are encoded from operons that are highly homologous, and it was an interesting observation that they

Table 2 Parameter values of S, P, and type 1 pili

Strain	IHE3034	IHE3034	HB101	HB101	HB101	HB101	HB101	HB101
Plasmid	–	–	pAZZ50	pANN801-13	pAES7	pAES8	pPAP5	pPKL4
Pili	$S_{II(wt)}$	Type $1_{(wt)}$	S_{II}	$S_{I(sfaX\ truncated)}$	$S_{II(sfaX::kan)}$	$S_{II(\Delta sfaX)}$	P[a]	Type 1[b]
F_{uf} (pN)[c]	26 ± 1	32 ± 3	26 ± 1	21 ± 2	24 ± 1	24 ± 1	28 ± 2	30 ± 2
Exp. I	28 ± 1		26 ± 1	19 ± 1	24 ± 1	25 ± 1		
Exp. II	26 ± 1		27 ± 1	22 ± 1	24 ± 2	25 ± 1		
Exp. III	26 ± 1		27 ± 1	20 ± 1	24 ± 1	23 ± 1		
ΔV_{AB} (kT)	35 ± 5	40 ± 7	37 ± 5	28 ± 5	33 ± 5	33 ± 5	24 ± 1	37 ± 2
Δx_{AT} (nm)	0.66 ± 0.08	0.56 ± 0.03	0.66 ± 0.08	0.56 ± 0.14	0.74 ± 0.09	0.67 ± 0.04	0.76 ± 0.11	0.59 ± 0.06
k_{AB}^{th} (Hz)	0.8 ± 0.4	0.012 ± 0.004	1.3 ± 0.9	8.8 ± 5.3	0.8 ± 0.5	0.9 ± 0.6	0.8 ± 0.5	0.016 ± 0.009
$\dot{L}*$ (nm/s)	200 ± 50	6 ± 2	450 ± 150	700 ± 100	280 ± 70	220 ± 50	400 ± 100	6 ± 3

[a] References (Andersson et al. 2006a, c)

[b] Reference (Andersson et al. 2007)

[c] Mean values of data from at least three experiments as described in Fig. 2. To illustrate the reproducibility we show the individual data sets from three separate experiments (Exps. I–III) in case of the S pili measurements

showed a difference regarding the force needed to rupture the layer-to-layer interaction in the rod and a seven-fold difference in kinetics. One possible reason for these differences could be that the few differences in amino acid sequence of the SfaA pilin subunits would have an impact on the biophysical properties monitored here. An alternative possibility became evident when we examined the Sfa clones in more detail and found–by nucleotide sequencing of the distal end of the sfa_I gene cluster in plasmid pANN801-13–that it is lacking about 40% of the $sfaX_I$ gene in contrast to the pAZZ50 clone that carries a complete gene cluster including the $sfaX_{II}$ gene (Fig. 1b). Both clinical isolates carry intact *sfaX* alleles in the *sfa* operons on their chromosomes, sfa_I in case of the UPEC isolate 536 (Brzuszkiewicz et al. 2006) and sfa_{II} in case of the NMEC isolate IHE3034 (Sjöström et al. 2009b).The $sfaX_{II}$ gene has recently been shown to be part of the major *sfa* gene operon (Sjöström et al. 2009b). The SfaX protein belongs to a family of MarR-like regulatory proteins. Our studies have shown that expression of the $sfaX_{II}$ gene affects motility by down regulation of flagella biosynthesis, and similar findings were reported for the largely homologous *papX* gene of a UPEC strain (Simms and Mobley 2008; Sjöström et al. 2009a). It was also found that $sfaX_{II}$ expression affected the DNA phase variation process leading to OFF status of the type 1 fimbrial expression (Sjöström et al. 2009a). However, while no effect on the expression of S_{II} pili was detected, its potential role for some steps in pili biogenesis, by being a part of the S_{II} pili operon, has not been ruled out (Sjöström et al. 2009b). This prompted us to directly test if expression of the $sfaX_{II}$ gene might affect the biomechanical features and the physical properties of the pili and thereby be a component involved in the differences observed between S_I and S_{II} pili. Therefore, we constructed mutant derivatives of the S_{II} pili clone such that we could perform measurements with pili expressed from bacteria lacking the $sfaX_{II}$ gene.

The plasmids pAES8 and pAES7 are identical to pAZZ50 except that the $sfaX_{II}$ gene is mutated either by partial deletion or by a Km-cassette insertion, respectively (Fig. 1b). Force-extension measurement, see Fig. 2e,f, right panels, of pili expressed by the two $sfaX_{II}$ mutated variants indicated that the average steady-state unfolding force was 24 ± 1 pN and 24 ± 2 pN, respectively. The thermal bond opening rate and the bond length were assessed to 0.9 ± 0.6 Hz, 0.67 ± 0.04 nm and 0.8 ± 0.5 Hz, 0.74 ± 0.09 nm, respectively.

As is shown in Table 2, there was good reproducibility in the experiments performed on different occasions, and the results indicate that there could be minor biomechanical differences between the S_{II} pili expressed from the $sfaX_{II}$ gene mutant derivatives and from the complete (pAZZ50) clone. The latter unfolded at 26 ± 1 pN with a thermal bond opening rate of 1.3 ± 0.9 Hz and a bond length of 0.66 ± 0.08 nm. It is not ruled out that the difference observed might be due, for example, to a regulatory role of the SfaX protein that might affect the biogenesis at the level of subunit stoichiometry and/or the assembly process. Recent findings regarding the role of SfaX in regulation at the transcriptional level of type 1 pili and flagella expression suggest that it is unlikely that the $SfaX_{II}$ protein would be incorporated into the S_{II} pili structures (Sjöström et al. 2009a). The $sfaX_{II}$ gene product shows homology to other regulatory proteins possessing DNA-binding properties, and its predicted secondary structure appears different from the S pili subunit proteins (data not shown). It remains to be elucidated at what level the SfaX proteins possibly may affect the S pili biomechanical properties.

Difference of unfolding/refolding dynamics among pili

As assessed previously and in this work, pili of the helix-like family show similar force-extension/contraction responses attributable to the geometrical shape and the similarity of the subunits. However, the force needed to unravel the quaternary structures and the dynamics of pili are slightly different. A comparison of the kinetics and the steady-state force of P, type 1, S_I, and S_{II} pili is shown in Fig. 4. As seen in the figure, they show major differences in their *relaxation* behavior, i.e., the transition time from a dynamic to a steady-state force response. The kinetics of S_I and S_{II} pili are similar to P pili, but the steady-state forces are lower. However, for type 1 pili the kinetics are significantly slower, whereas the steady-state force is slightly higher in comparison to the other three. We have summarized in Table 2 the results of this study and the parameter values assessed from our earlier studies of P and type 1 pili.

Comparison between $SfaA_I$ and $SfaA_{II}$

The small genetic variation between $SfaA_I$ and $SfaA_{II}$, ~20%, and the identical three-dimensional helix-like structure point towards minor differences in the biomechanical properties. Using force-measuring optical tweezers in situ measurements, we have shown that the force-extension response of these two fimbria is identical. They can be unfolded to a linearized polymer and reversibly be refolded back to its original structure. This action can be performed without any indication of plasticity or fatigue that is similar to P pili (Andersson et al. 2006b). However, the force required to unravel the helix-like structures (quaternary) is slightly dissimilar. S_{II} pili expressed by NMEC seem to have stronger layer-to-layer interactions compared to S_I pili expressed by UTI.

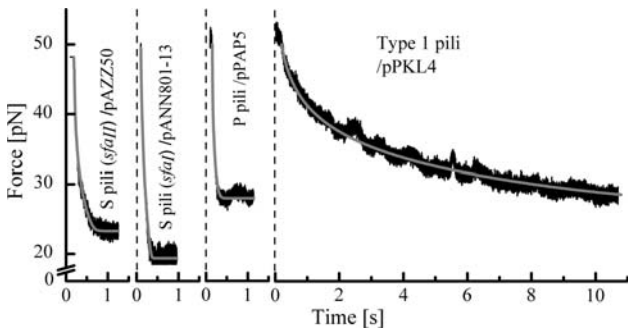

Fig. 4 Relaxation data curves from S_I, S_{II}, P, and type 1 pili fitted with Eq. 4. Each set of data is plotted with an individual X-axis (abscissa) with a truncated Y-axis. Data for P pili and type 1 pili were taken from earlier published results (Andersson et al. 2006a, c; Andersson et al. 2007). Differences in the kinetic behavior and the final steady-state force level are clearly seen

It has been shown, and is further discussed below, that *E. coli* expressing type 1 pili increases its adhesion time when exposed to shear forces induced by a flow (Thomas et al. 2002). Also, it is believed that the shaft of the pilus has coevolved with the adhesin for optimized performance. Thus, we suggest that a difference in unraveling force of the two S pili might be correlated to in vivo environmental forces generated by natural flows, such as urine and blood flows. Moreover, the kinetic differences, i.e., the speed at which a subunit in the helix-like rod opens/closes, of the two pili can presumably be addressed to the variation in shear flow rates within the urinary tract or blood–brain barrier. However, verifying this hypothesis requires detailed information regarding the in vivo shear forces and shear rates that can improve the knowledge regarding how the development and expression of pili helps bacteria to optimize adhesion under different environmental conditions. For such a study, S_I and S_{II} pili, which are correlated to different in vivo environments, could be a suitable model system since they have been characterized with respect to their genetic and structural compositions and now also for their force and kinetic responses.

We also wish to point out that this work verifies that pili encoded from a unique operon but expressed by two different bacterial strains (the clinical isolate IHE3034 and the laboratory strain HB101) do not show any biomechanical differences in terms of bond length, steady-state unfolding force, and corner velocity. It is therefore justified to use HB101 as a model host for single pili force studies since they do not express any native pili that could interfere. In addition, by performing force measurements it is possible to identify pili expressed by bacteria through the characteristic response that each specific variety exhibits.

Comparison between different types of pili

In general, class I adhesion pili appear to have the same force-extension response, although different parameter values for bond length, bond strength, and kinetics have been assessed. Previous force-extension results on both P and type 1 pili indicated a major kinetic difference between the two (Andersson et al. 2007). It was shown that the relaxation time of a single pilus from a dynamic regime (50 pN) is ~35 times slower for type 1 than for P pili, i.e., about 7 s compared to 0.2 s, respectively. In addition, S_I pili correlated to UTI (pANN801-13) show ~10 times faster kinetics than P pili and ~550 times faster kinetics than type 1 pili. So far, we do not have any good explanation for why S pili exhibit such fast kinetics.

The dissimilarity in the dynamic response of P and type 1 pili can hypothetically be addressed to the different properties of the flow in the surrounding of a bacteria in vivo. For example, it is known that the urine is transported

in boluses via ureters by peristaltic activity from the kidney to the bladder (Griffiths 1987; Griffiths et al. 1987) and that the bladder expels urine via the urethra (Ozawa et al. 1998). The peristaltic waves in the ureters, which occur at a rate of approximately 3.3 min^{-1} (Davenport et al. 2007), generate flow recirculation (Vogel et al. 2004). The flow in the bolus interacting with bacteria thereby results in a high variation of shear rates, as well as perpendicular and reversal wall shear forces (Vogel et al. 2004) similar to those in the ileum (Jeffrey et al. 2003). These forces must be damped by a structure that absorbs and relaxes in a optimum way in order to maintain firm adhesion, i.e., relax fast to minimize the load of the adhesin and thereby extend the lifetime of a slip bond, such as the adhesin of P pili (Björnham et al. 2009), or slow, to maintain the load at reasonable levels for a catch bond, such as the adhesin of type 1 pili (Forero et al. 2006; Nilsson et al. 2006; Thomas et al. 2002). Since it is hypothesized that the adhesin and the rod have coevolved, it is likely that the rod evolved to optimize the function of the adhesin. Therefore, it might be possible that the relaxation behavior of the aforementioned pili could be addressed to the lifetime of such adhesins. It thereby remains as a future work to characterize the properties of the S pili adhesin.

Acknowledgments This paper is dedicated to our colleague and friend Dr. Erik Fällman. The authors thank Prof. Ove Axner for valuable discussions and Monica Persson for assistance with the preparations of bacteria and AFM imaging. This work was performed within the Umeå Centre for Microbial Research (UCMR) and was carried out in the frame of the European Virtual Institute for Functional Genomics of Bacterial Pathogens (CEE LSHB-CT-2005-512061) and the ERA-NET project "Deciphering the intersection of commensal and extraintestinal pathogenic *E. coli*" with support by grants from the Swedish Research Council. We acknowledge economic support for the construction of force-measuring optical tweezers system from the Kempe foundation and from Magnus Bergvall's foundation. The "Fondation Pour La Recherche Médicale" is also acknowledged for the French post-doctoral fellowship awarded to M.C. (grant no. SPE20071211235).

References

Andersson M, Fällman E, Uhlin BE, Axner O (2006a) Dynamic force spectroscopy of the unfolding of P pili. Biophys J 91:2717–2725

Andersson M, Fällman E, Uhlin BE, Axner O (2006b) Force measuring optical tweezers system for long time measurements of pili stability. SPIE 6088:286–295

Andersson M, Fällman E, Uhlin BE, Axner O (2006c) A sticky chain model of the elongation of *Escherichia coli* P pili under strain. Biophys J 90:1521–1534

Andersson M, Uhlin BE, Fällman E (2007) The biomechanical properties of *E.* coli pili for urinary tract attachment reflect the host environment. Biophys J 93:3008–3014

Andersson M, Axner O, Almqvist F, Uhlin BE, Fällman E (2008) Physical properties of biopolymers assessed by optical tweezers: Analysis of folding and refolding of bacterial pili. Chem Phys Chem 9:221–235

Balsalobre C, Morschhaüser J, Jass J, Hacker J, Uhlin BE (2003) Transcriptional analysis of the *sfa* determinant revealing multiple mRNA processing events in the biogenesis of S fimbriae in pathogenic *Escherichia coli*. J Bacteriol 185:620–629

Berger H, Hacker J, Juarez A, Hughes C, Goebel W (1982) Cloning of the chromosomal determinants encoding hemolysin production and mannose-resistant hemagglutination in *Escherichia coli*. J Bacteriol 152:1241–1247

Berglund J, Knight SD (2003) Structural basis for bacterial adhesion in the urinary tract. Glycobiol Med 535:33–52

Björnham O, Nilsson H, Andersson M, Schedin S (2009) Physical properties of the specific PapG-galabiose binding in *E.* coli P pili-mediated adhesion. Eur Biophys J 38:245–254

Boyer HW, Roulland D (1969) A complementation analysis of restriction and modification of DNA in *Escherichia Coli*. J Mol Biol 41:459–472

Brzuszkiewicz E, Brüggemann H, Liesegang H, Emmerth M, Ölschläger T, Nagy G, Albermann K, Wagner C, Buchrieser C, Emödy L, Gottschalk G, Hacker J, Dobrindt U (2006) How to become a uropathogen: comparative genomic analysis of extraintestinal pathogenic *Escherichia coli* strains. Proc Natl Acad Sci USA 103:12879–12884

Corpet F (1988) Multiple sequence alignment with hierarchical-clustering. Nucleic Acids Res 16:10881–10890

Davenport K, Timoney AG, Keeley FX Jr (2007) Effect of smooth muscle relaxant drugs on proximal human ureteric activity in vivo: a pilot study. Urol Res 35:207–213

Duncan MJ, Mann EL, Cohen MS, Ofek I, Sharon N, Abraham SN (2005) The distinct binding specificities exhibited by enterobacterial type 1 fimbriae are determined by their fimbrial shafts. J Biol Chem 280:37707–37716

Fällman E, Schedin S, Jass J, Andersson M, Uhlin BE, Axner O (2004) Optical tweezers based force measurement system for quantitating binding interactions: system design and application for the study of bacterial adhesion. Biosens Bioelectron 19:1429–1437

Fällman E, Schedin S, Jass J, Uhlin BE, Axner O (2005) The unfolding of the P pili quaternary structure by stretching is reversible, not plastic. EMBO Rep 6:52–56

Forero M, Yakovenko O, Sokurenko EV, Thomas WE, Vogel V (2006) Uncoiling mechanics of *Escherichia coli* Type I fimbriae are optimized for catch bonds. PLoS Biol 4:1509–1516

Griffiths DJ (1987) Dynamics of the upper urinary-Tract.1. Peristaltic flow through a distensible tube of limited length. Phys Med Biol 32:813–822

Griffiths DJ, Constantinou CE, Mortensen J, Djurhuus JC (1987) Dynamics of the upper urinary-Tract.2. The effect of variations of peristaltic frequency and bladder pressure on pyeloureteral pressure/flow relations. Phys Med Biol 32:823–833

Guyer MS, Reed RR, Steitz JA, Low KB (1980) Identification of a sex-factor-affinity site in *Escherichia coli* as gamma-delta. Cold Spring Harb Symp Quant Biol 45:135–140

Guzman LM, Belin D, Carson MJ, Beckwith J (1995) Tight regulation, modulation, and high-level expression by vectors containing the arabinose P_{BAD} promoter. J Bacteriol 177:4121–4130

Hacker J, Schmidt G, Hughes C, Knapp S, Marget M, Goebel W (1985) Cloning and characterization of genes involved in production of mannose-resistant, neuraminidase-susceptible (X) fimbriae from a Uropathogenic O6–K15-H31 *Escherichia coli* strain. Infect Immun 47:434–440

Hacker J, Kestler H, Hoschützky H, Jann K, Lottspeich F, Korhonen TK (1993) Cloning and characterization of the S-Fimbrial Adhesin-Ii complex of an *Escherichia coli* O-18–K1 meningitis isolate. Infect Immun 61:544–550

Holden NJ, Gally DL (2004) Switches, cross-talk and memory in *Escherichia coli* adherence. J Med Microbiol 53:585–593

Jass J, Schedin S, Fällman E, Ohlsson J, Nilsson U, Uhlin BE, Axner O (2004) Physical properties of *Escherichia coli* P pili measured by optical tweezers. Biophys J 87:4271–4283

Jeffrey B, Udaykumar HS, Schulze KS (2003) Flow fields generated by peristaltic reflex in isolated guinea pig ileum: impact of contraction depth and shoulders. Am J Physiol Gastrointest Liver Physiol 285:G907–G918

Klemm P, Jørgensen BJ, Vandie I, Deree H, Bergmans H (1985) The *fim* genes responsible for synthesis of Type-1 fimbriae in *Escherichia coli*, cloning and genetic organization. Mol Gen Genet 199:410–414

Knight SD, Choudhury D, Hultgren S, Pinkner J, Stojanoff V, Thompson A (2002) Structure of the S pilus periplasmic chaperone SfaE at 2.2 ångström resolution. Acta Crystallogr D Biol Crystallogr 58:1016–1022

Korhonen TK, Valtonen MV, Parkkinen J, Vaisanenrhen V, Finne J, Ørskov F, Ørskov I, Svenson SB, Mäkelä PH (1985) Serotypes, hemolysin production, and receptor recognition of *Escherichia coli* strains associated with neonatal sepsis and meningitis. Infect Immun 48:486–491

Lugmaier RA, Schedin S, Kühner F, Benoit M (2008) Dynamic restacking of *Escherichia coli* P-pili. Eur Biophys J 37:111–120

Lund B, Lindberg F, Marklund BI, Normark S (1987) The PapG protein is the alpha-D-Galactopyranosyl-(1–4)-Beta-D-galactopyranose-binding adhesin of uropathogenic *Escherichia coli*. Proc Natl Acad Sci USA 84:5898–5902

Lund B, Marklund BI, Strömberg N, Lindberg F, Karlsson KA, Normark S (1988) Uropathogenic *Escherichia coli* can express serologically identical Pili of different receptor-binding specificities. Mol Microbiol 2:255–263

Miller E, Garcia TI, Hultgren S, Oberhauser A (2006) The mechanical properties of *E. coli* Type 1 Pili measured by atomic force microscopy techniques. Biophys J 91:3848–3856

Nilsson LM, Thomas WE, Trintchina E, Vogel V, Sokurenko EV (2006) Catch bond-mediated adhesion without a shear threshold—trimannose versus monomannose interactions with the FimH adhesin of *Escherichia coli*. J Biol Chem 281:16656–16663

Old D (1972) Inhibition of interaction between fimbrial hemagglutinins and erythrocytes by D-mannose and other carbohydrates. J Gen Microbiol 71:149–157

Ozawa H, Kumon H, Yokoyama T, Watanabe T, Chancellor MB (1998) Development of noninvasive velocity flow video urodynamics using doppler sonography. part ii: clinical application in bladder outlet obstruction. J Urol 160:1792–1796

Parkkinen J, Rogers GN, Korhonen T, Dahr W, Finne J (1986) Identification of the O-Linked sialyloligosaccharides of glycophorin-a as the erythrocyte receptors for S-Fimbriated *Escherichia coli*. Infect Immun 54:37–42

Pouttu R, Westerlund-Wikström B, Lång H, Alsti K, Virkola R, Saarela U, Siitonen A, Kalkkinen N, Korhonen TK (2001) *matB*, a common fimbrillin gene of *Escherichia coli*, expressed in a genetically conserved, virulent clonal group. J Bacteriol 183:4727–4736

Sambrook J, Russel DW (2001) Molecular cloning: a laboratory manual. 3 ed

Sauer FG, Fütterer K, Pinkner JS, Dodson KW, Hultgren SJ, Waksman G (1999) Structural basis of chaperone function and pilus biogenesis. Science 285:1058–1061

Selander RK, Korhonen TK, Väisänen-Rhen V, Williams PH, Pattison PE, Caugant DA (1986) Genetic-relationships and clonal structure of strains of *Escherichia coli* causing neonatal septicemia and meningitis. Infect Immun 52:213–222

Simms AN, Mobley HLT (2008) PapX, a P Fimbrial operon-encoded inhibitor of motility in uropathogenic *Escherichia coli*. Infect Immun 76:4833–4841

Sjöström AE, Balsalobre C, Emödy L, Westerlund-Wikström B, Hacker J, Uhlin BE (2009a) The $SfaX_{II}$ protein from newborn meningitis *E. coli* is involved in regulation of motility and type 1 fimbriae expression. Microb Pathog 46:243–252

Sjöström AE, Sondén B, Müller C, Rydström A, Dobrindt U, Wai SN, Uhlin BE (2009b) Analysis of the $sfaX_{II}$ locus in the *Escherichia coli* meningitis isolate IHE3034 reveals two novel regulatory genes within the promoter-distal region of the main S fimbrial operon. Microb Pathog 46:150–158

Thomas WE, Trintchina E, Forero M, Vogel V, Sokurenko EV (2002) Bacterial adhesion to target cells enhanced by shear force. Cell 109:913–923

Vogel A, Elmabsout B, Gintz D (2004) Modelling of urine flow in an ureteral bolus. C R Mec 332:737–742

Wright KJ, Hultgren SJ (2006) Sticky fibers and uropathogenesis: bacterial adhesins in the urinary tract. Future Microbiol 1:75–87